0026-895X/02/6202-334–342$7.00
MOLECULAR PHARMACOLOGY
Copyright © 2002 The American Society for Pharmacology and Experimental Therapeutics
Mol Pharmacol 62:334–342, 2002

Vol. 62, No. 2
1549/997076
Printed in U.S.A.

A Polymorphism in the Mouse Neuronal α4 Nicotinic Receptor Subunit Results in An Alteration in Receptor Function

PETER DOBELIS, MICHAEL J. MARKS, PAUL WHITEAKER, SETH A. BALOGH, ALLAN C. COLLINS, and JERRY A. STITZEL

Institute for Behavioral Genetics, University of Colorado, Boulder, Colorado (P.D., M.J.M., P.W., S.A.B., A.C.C.); Department of Pharmacology, University of Colorado Health Sciences Center, Denver, Colorado (P.D.); and Department of Pharmacology, University of Michigan, Ann Arbor, Michigan (J.A.S.)

Received December 17, 2001; accepted April 26, 2002

This article is available online at http://molpharm.aspetjournals.org

ABSTRACT

Nicotine-stimulated $^{86}Rb^{+}$ efflux and [^{3}H]cytisine binding, both of which seem to measure the nicotinic acetylcholine receptor, composed of α4 and β2 subunits, were assessed in eight brain regions obtained from 14 inbred mouse strains. The potential role of a single nucleotide polymorphism (SNP) in the nicotinic receptor α4 subunit gene (Chrna4) on nicotinic receptor binding and function in mice was also evaluated. This SNP leads to an alanine-to-threonine variation at amino acid position 529 of the nascent α4 subunit polypeptide. Both nicotine-stimulated $^{86}Rb^{+}$ efflux and [^{3}H]cytisine binding were found to vary across brain regions and among mouse strains. Variability in nicotine-stimulated $^{86}Rb^{+}$ efflux was positively correlated ($r > 0.9$) within each strain with the number of [^{3}H]cytisine binding sites. However, the number of [^{3}H]cytisine binding sites was not correlated with nicotine-stimulated $^{86}Rb^{+}$ efflux across mouse strains. In contrast, the Chrna4 polymorphism was associated with receptor function across mouse strains: $^{86}Rb^{+}$ efflux was greater in seven of the eight brain regions studied in those mouse strains that carry the Ala-529 variant of Chrna4. The Chrna4 SNP did not seem to influence the number of [^{3}H]cytisine binding sites across mouse strains. These data indicate that inbred mouse strains exhibit differences in receptor function that cannot be attributed to variation in receptor expression but may be explained, at least in part, by the missense polymorphism in the α4 subunit.

Inbred and selectively bred mouse strains differ in what may be components of the nicotine addiction process. For example, inbred mouse strains differ in oral self-administration of nicotine (Meliska et al., 1995; Robinson et al., 1996), in sensitivity to a first dose of nicotine (Hatchell and Collins, 1977; Marks et al., 1989; Miner and Collins, 1989; Flores et al., 1999), in the development of tolerance aftera first dose (de Fiebre and Collins, 1988), and in the development of tolerance with chronic treatment (Marks et al., 1991). These strain differences are not readily explained by differences in nicotine metabolism (Hatchell and Collins, 1977), but differences in nicotinic receptor numbers may contribute to the variation in response to nicotine. For example, in an analysis that used 19 inbred mouse strains, significant negative correlations were found between the number of [^{3}H]nicotine binding sites and ED_{50}-like values for the effects of nicotine on several measures, particularly locomotor activities and body temperature (Marks et al., 1989). Studies done with nAChR α4 (Marubio et al., 1999) and β2 (Picciotto et al., 1995) subunit null mutant mice, as well as immunological studies (Whiting and Lindstrom, 1987; Flores et al., 1992), indicate that in most brain regions, nicotine binds with high affinity to receptors made up of α4 and β2 subunits. Thus, the finding that variation in the number of [^{3}H]nicotine binding sites is significantly correlated ($r = -0.63$) with variability in sensitivity to the effects of nicotine on locomotor activity and body temperature implies that these responses to nicotine may be modulated by nicotinic receptors that include the α4 and β2 subunits.

Recently, a single nucleotide polymorphism (SNP) in the α4 subunit cDNA was identified between the selected mouse lines, long-sleep (LS) and short-sleep (SS) (Stitzel et al., 2001). The SNP predicts a threonine/alanine variation at amino acid position 529 of the α4 subunit cDNA. Several behavioral and physiological responses to nicotine have been found to be associated with this SNP as well as with a

This work was supported by grants from the National Institute on Alcohol Abuse and Alcoholism (AA11156) and National Institute on Drug Abuse (DA00197 and DA10156 to A.C.C.) and funds from the National Institute on Drug Abuse (DA14369), Alcoholic Beverage Medical Research Foundation, the University of Michigan Tobacco Research Network (to J.A.S.), National Institutes of Mental Health (MH61617), and Colorado Tobacco Research Program (IF-059) (to P.D.).

ABBREVIATIONS: nAChR, nicotinic acetylcholine receptor; Chrna4, cholinergic receptor, nicotinic α4 subunit gene; LS, long-sleep; SS, short-sleep; SNP, single nucleotide polymorphism; ANOVA, analysis of variance; CX, cortex; SE, septum; HP, hippocampus; ST, striatum; HT, hypothalamus; TH, thalamus; MB, midbrain; HB, hind brain; RI, recombinant inbred.

restriction fragment-length polymorphism in the α4 subunit gene, Chrna4 (Stitzel et al., 2000; Tritto et al., 2002), and initial studies have indicated that this amino acid variation at position 529 may have functional consequences (Stitzel et al., 2001). Therefore, mouse strain differences in sensitivity to nicotine might be influenced not only by individual differences in the numbers of α4-containing receptors but also by individual variability in receptor function.

The functional properties of nicotinic receptors, which are ligand-gated ion channels, are frequently measured using electrophysiological methods. However, a neurochemical assay that measures receptor function by monitoring nicotinic agonist-stimulated $^{86}Rb^+$ efflux from synaptosomes has also been used (Marks et al., 1993). Partially because maximal nicotine-stimulated ion flux was highly ($r = 0.99$) correlated with the number of [^{3}H]nicotine binding sites across eight brain regions, it was tentatively concluded that the receptor that modulates this response is an $\alpha4\beta2$ receptor. Additional support that nicotine-stimulated ion flux is modulated by $\alpha4\beta2$ receptors arises from the observation that $^{86}Rb^+$ flux was significantly reduced, or lost, in most brain regions obtained from homozygous $\beta2$ null mutant mice (Marks et al., 2000; Whiteaker et al., 2000) and the observations that agonist potencies and efficacies, antagonist specificities, and desensitization properties (Marks et al., 1994, 1996) resemble those of $\alpha4\beta2$-type receptors expressed in oocytes and cell lines (Gross et al., 1991; Luetje and Patrick, 1991; Whiting et al., 1991; Buisson et al., 1996; Sabey et al., 1999).

The recent observation that nicotine-stimulated $^{86}Rb^+$ efflux differs in synaptosomes prepared from LS and SS thalamic tissue further supports the assertion that the α4 subunit is a component of the nAChR that modulates the $^{86}Rb^+$ efflux process (Stitzel et al., 2001). However, there are many differences between the LS and SS mouse lines that might contribute to the difference in nicotine-stimulated $^{86}Rb^+$ efflux. Consequently, additional studies are needed to evaluate the hypothesis that the missense polymorphism in the α4 receptor subunit leads to a difference in nicotine-stimulated ion flux. This report describes the results of studies that evaluated nicotine-stimulated $^{86}Rb^+$ efflux in eight brain regions derived from 14 inbred mouse strains and assessed the potential effects of the α4 subunit polymorphism on receptor function and expression.

Experimental Procedures

Materials. Carrier-free ^{86}RbCl (1–100 Ci/ml) and [^{3}H]cytisine (38.5 Ci/mmol) were purchased from PerkinElmer Life Sciences (Boston, MA). Budget Solve (Research Products International, Mt. Prospect, IL) was used as scintillation cocktail to measure [^{3}H] in the binding assays. Unless specified, all other chemicals were purchased from Sigma-Aldrich (St. Louis, MO).

Mice. Male mice of 14 inbred strains were used in this study. Mice of the A/J/Ibg, BALB/cByJ/Ibg, C3H/2/Ibg, C57BL/6J, DBA/2J/Ibg, and 129 SvEv/Tac strains were bred at the Institute for Behavioral Genetics (University of Colorado, Boulder, CO). These strains have been maintained in our vivarium for at least 10 generations. All mice were weaned at 25 days of age and housed with male littermates. Mice were 60 to 90 days old when tested. Male mice of the following strains were purchased from The Jackson Laboratories (Bar Harbor, ME): AKR/J, BUB/BnJ, CBA/J, C57BL/10J, C57BR/cdJ, C58/J, DBA/1J, and RIIIS/J. All mice were 4 to 6 weeks old when they were received and were housed five per cage in our mouse colony until they were 60 to 90 days old. A 12-h light/dark cycle was maintained, and the mice were given free access to food (Wayne Lab Blox; Wayne Feed Division, Chicago, IL) and water. The animal protocols used in the studies reported here were reviewed and approved by the National Institutes of Health-approved Institutional Animal Care and Use Committee of the University of Colorado.

Preparation of Crude Synaptosomes. Each mouse was killed by cervical dislocation. Its brain was removed, placed on an ice-cold platform, and dissected into the following regions: cerebral cortex, thalamus, hippocampus, striatum, hindbrain (pons and medulla), midbrain, septum, and hypothalamus. The brain regions were placed in 10 volumes of ice-cold 0.32 M sucrose buffered to pH 7.5 with 5 mM HEPES hemisodium and homogenized by hand using a Potter-Elvehjem Teflon/glass tissue homogenizer (Kimble/Kontes, Vineland, NJ). The homogenate was centrifuged at 500*g* for 10 min. The resulting supernatant was harvested and centrifuged at 12,000*g* for 20 min. The tissue pellet (P2) derived from this centrifugation step was harvested and resuspended in load buffer (140 mM NaCl, 1.5 mM KCl, 2.0 mM $CaCl_2$, 1.0 mM $MgCl_2$, 25 mM HEPES hemisodium salt, and 20 mM glucose, pH 7.5).

$^{86}Rb^+$ Uptake. Crude synaptosomes were loaded with $^{86}Rb^+$ by incubation for 30 min at 22°C. The final incubation volume of 35 μl per sample contained approximately 4 μCi of $^{86}Rb^+$. After the 30-min incubation period, the crude synaptosomes were collected by gentle vacuum (−10,132.5 Pa) filtration onto 6-mm glass fiber filters (type GC; Advantec MFS, Inc., Dublin, CA) followed by three washes with 0.5 ml of load buffer.

General Perfusion Method. Each 6-mm filter containing synaptosomes was placed on a 13-mm glass fiber filter mounted on a polypropylene platform. The perfusion apparatus has been described in more detail previously (Marks et al., 1993). Perfusion buffer was subsequently passed over the tissue at a rate of 3.0 ml/min. The composition of the perfusion buffer was 135 mM NaCl, 1.5 mM KCl, 5.0 mM CsCl, 2.0 mM $CaCl_2$, 1.0 mM $MgSO_4$, 1 g/l bovine serum albumin, 50 nM tetrodotoxin, 25 mM HEPES hemisodium salt, and 20 mM glucose, pH 7.5. The synaptosomes were perfused for 5 min before samples were collected. Samples were then collected in 12 × 75-mm test tubes at 30-s intervals. The samples were collected for 5 min, and nicotine stimulation was for 1 min. In most instances (except for the concentration-response curves for the 129SvEv and A/J strains), 10 μM nicotine was used for stimulation. Previous studies (Marks et al., 1999, 2000) have shown that $^{86}Rb^+$ efflux is mediated by two pharmacologically distinct components with different agonist affinities. The high-affinity component is maximally activated by 10 μM nicotine and is believed to be mediated by the $\alpha4\beta2$ receptor subtype. The low-affinity component is mediated by a receptor or receptors of unknown composition and is not activated by 10 μM nicotine. Consequently, the use of 10 μM nicotine in these studies allowed maximal stimulation of the high-affinity component while avoiding activation of the low-affinity response.

The radioactivity was counted with a gamma counter (Cobra Auto-Gamma counting system; PerkinElmer Life Sciences). The amount of agonist-stimulated release was calculated as the percentage of total tissue $^{86}Rb^+$ content by subtracting the extrapolated baseline release from the nicotine-stimulated release and dividing this number by the amount of $^{86}Rb^+$ in the tissue sample, measured after perfusion was complete, as described previously (Marks et al., 1993, 2000).

[^{3}H]Cytisine Binding. The binding of [^{3}H]cytisine to particulate fractions from the eight brain regions was measured using methods similar to those described for [^{3}H]nicotine binding in Marks et al. (1993). Particulate fractions obtained from P2 preparations of the eight brain regions were incubated with 10 nM [^{3}H]cytisine in 100 μl of load buffer for at least 45 min at 22°C. Incubations were conducted in 96-well polystyrene plates. Nonspecific binding was determined by including 10 μM unlabeled (−) nicotine in the incubation. The binding reaction was terminated by filtration of the protein onto glass fiber filters that had been treated with 0.5% polyethylenimine in load buffer. After filtration, the filters were washed six times with

ice-cold load buffer. The filters were collected and placed in scintillation vials. After the addition of scintillation fluid, the radioactivity was measured using a β-scintillation counter (Tri-Carb Scintillation Analyzer; PerkinElmer Life Sciences). Homogenate protein levels were determined as described elsewhere (Marks et al., 1991).

Chrna4 Genotyping. Genomic DNA from the 14 inbred strains was either isolated from splenic tissue by standard proteinase K digestion/phenol extraction methodology as described previously (Stitzel et al., 2000) or purchased from The Jackson Laboratories. A region of Chrna4 that spanned the SNP at nucleotide position 1587 was amplified by a reaction that included 50 ng of genomic DNA, 1× PCR buffer II (Applied Biosystems, Foster City, CA), 2.5 mM $MgCl_2$, 200 μM each of dGTP, dATP, dCTP, and dTTP, 20 pmol of each amplification primer (5′-GGTCCCTGAGCGTCCAGCATG-3′ and 5′-GGTCCTATCTGGGTCGGGGTG-3′), and 2.5 units of AmpliTaq Gold DNA polymerase (Applied Biosystems) in a reaction volume of 50 μl. Amplification of the DNA was accomplished using a touchdown protocol with an initial annealing temperature of 65°C and final amplification conditions of 94°C for 30 s, 55°C for 30 s, and 72°C for 1 min, for 30 cycles. This amplification reaction generates a product of 405 base pairs that spans from 185 base pairs upstream of the Chrna4 SNP at nucleotide position 1587 to 220 downstream of this SNP. After amplification, 5 μl of the PCR reaction was digested with *Stu*I in a final volume of 20 μl and subsequently electrophoresed on a 1.8% agarose gel. The restriction enzyme *Stu*I (recognition sequence AGGCCT) will cut the PCR product if the alanine codon, GCC, is present at codon position 529 but will not cut the PCR product if the threonine codon, ACC, is present at this position.

Statistical Analysis. Within-strain analysis of regional differences in $^{86}Rb^+$ efflux and [^{3}H]cytisine binding was assessed using one-way ANOVA. A two-way ANOVA followed by Duncan's post hoc test was used to assess strain and regional differences.

Results

Agonist-induced $^{86}Rb^+$ efflux from synaptosomal preparations has been used to measure nicotinic receptor function. Figure 1 presents the results of a typical efflux experiment. Exposure to nicotine elicited a concentration-dependent increase in $^{86}Rb^+$ efflux above the spontaneous (unstimulated) efflux. An earlier study (Marks et al., 1993) showed that nicotine-stimulated $^{86}Rb^+$ efflux may be measured in multiple brain regions, and this response is highly correlated across brain regions with the number of high-affinity nicotine binding sites. These studies were done using the inbred mouse strain C57BL/6. To determine whether $^{86}Rb^+$ efflux is correlated with high-affinity nicotine binding sites in other inbred mouse strains, these two measures were evaluated in the inbred mouse strains 129/SvEv and A/J. In initial experiments, $^{86}Rb^+$ efflux was measured in thalamic synaptosomes prepared from these two mouse strains. The thalamus was chosen for this preliminary assessment because previous studies (Marks et al., 2000) indicated that $^{86}Rb^+$ efflux in this brain region seems to be modulated by a single nicotinic receptor subtype made up of α4 and β2 subunits. As is evident in the data presented in Fig. 2, nicotine elicited a concentration-dependent increase in ion flux from thalamic synaptosomes prepared from both A/Ibg and 129SvEv mice. The two strains differed significantly ($p < 0.05$) in maximal nicotine-stimulated ion flux in thalamus: E_{max} was 2.96 ± 0.20 units in A/Ibg mice and 2.35 ± 0.16 units in 129SvEv mice. The EC_{50} values for nicotine-stimulated ion flux from thalamic synaptosomes were virtually identical for the two strains: 0.68 ± 0.17 μM for A/Ibg mice and 0.83 ± 0.21 μM for 129SvEv mice.

Subsequently, [^{3}H]cytisine binding and nicotine-stimulated $^{86}Rb^+$ efflux were measured in eight brain regions from the A and 129 strains. [^{3}H]Cytisine binding was measured using a concentration (10 nM) of the ligand that is much higher than the K_D value of 0.4 nM (Whiteaker et al., 2000). Therefore, these assays should provide an estimate of the maximal number of binding sites. A maximally activating concentration of nicotine (10 μM), selected from the results reported in Fig. 2, was used in the ion flux assays. The graphical and statistical results of these experiments are provided in Fig. 3. Figure 3A presents the binding data obtained with 129 SvEv mice. [^{3}H]Cytisine binding differed significantly across the brain regions. In some brain regions, such as the septum, [^{3}H]cytisine binding was low (approxi-

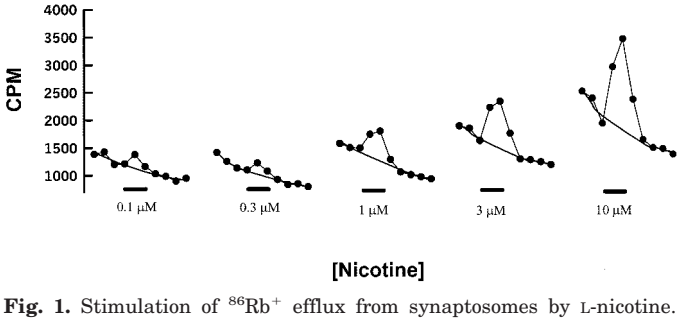

Fig. 1. Stimulation of $^{86}Rb^+$ efflux from synaptosomes by L-nicotine. Responses to a 1-min stimulation with nicotine are shown. The points in each trace represent 30-s fractions and are expressed in cpm. The solid bar under each trace indicates the presence of nicotine (1 min), and the concentration of nicotine is indicated under each bar. The solid line in each trace is an extrapolated baseline fit using an exponential function. The area under the baseline is subtracted from the total area under the trace to yield the amount of $^{86}Rb^+$ released in response to nicotine stimulation.

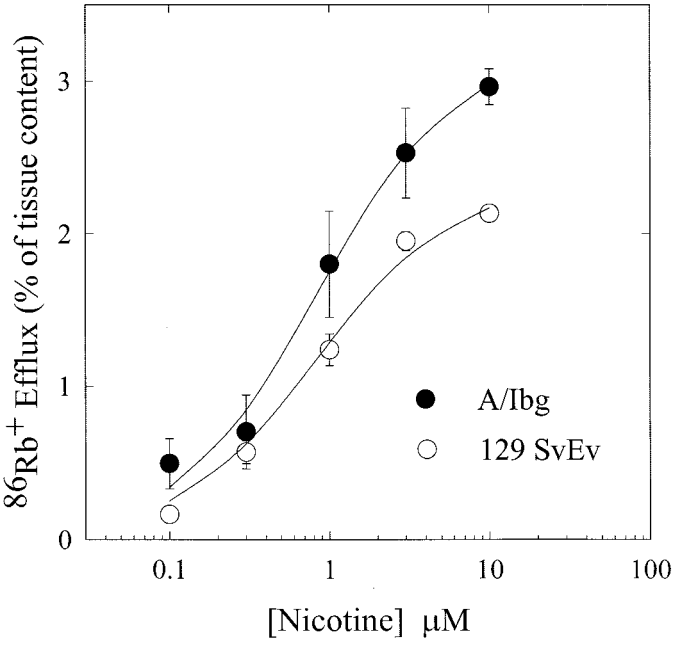

Fig. 2. Concentration-response relationship for nicotine-stimulated $^{86}Rb^+$ efflux in A/J and 129 SvEv mice. The concentration-response relationship for nicotine (1-min application) was determined in thalamic synaptosomes prepared from A/J and 129 SvEv mice. The EC_{50} values were 0.68 ± 0.17 μM and 0.83 ± 0.21 μM for A/J and 129 SvEv, respectively. These values were not significantly different. The E_{max} values were 2.96 ± 0.2 for A/J and 2.35 ± 0.16 for 129 SvEv and differed significantly ($p < 0.05$, Student's t test).

mately 50 fmol/mg protein), whereas in other brain regions, most notably thalamus, high levels of binding (nearly 200 fmol/mg protein) were detected. Figure 3B shows the $^{86}Rb^{+}$ efflux elicited by 10 μM nicotine in these same brain regions. The brain regions differed significantly in nicotine-stimulated ion flux. Figure 3C shows the relationship between [^{3}H]cytisine binding and nicotine-stimulated $^{86}Rb^{+}$ efflux using data from the 129 SvEv mice. Binding and ion flux were significantly correlated, i.e., more binding sites was associated with greater ion flux. The correlation coefficient of 0.94 suggests that approximately 88% (r^2) of the variance in ion flux across the brain regions is due to variability in the number of receptors that bind [^{3}H]cytisine with high affinity.

Figure 3, D and E presents the [^{3}H]cytisine binding (D) and nicotine-stimulated $^{86}Rb^{+}$ efflux (E) data obtained in these same brain regions obtained from A/Ibg mice. Both [^{3}H]cytisine binding and $^{86}Rb^{+}$ efflux differed significantly across brain regions. As is shown in Fig. 3F, these two measures were significantly correlated ($r = 0.93$), suggesting that approximately 86% of the variability in the amount of nicotine-stimulated ion flux may be due to variability in the number of [^{3}H]cytisine binding sites. As was the case with the 129 SvEv mice, higher binding was associated with more ion flux.

The two mouse strains were compared with respect to [^{3}H]cytisine binding and nicotine-stimulated $^{86}Rb^{+}$ efflux using data obtained from seven of the brain regions (septal data were deleted from this analysis because tissue was pooled from several animals to obtain an adequate signal). The two-way ANOVA of [^{3}H]cytisine binding detected a significant effect of brain region, as expected, but the two strains did not differ in binding in any of the regions. Analysis of the ion flux data detected significant overall effects of brain region and strain, and a significant strain-by-region interaction term was also obtained. The findings that the A/J and 129SvEv mouse strains did not differ substantially in binding, whereas significant differences in ion flux were found, suggest that the nicotinic receptor(s) that binds cytisine with high affinity differs in function between the two strains.

To evaluate further the relationship between [^{3}H]cytisine binding and $^{86}Rb^{+}$ efflux, this analysis was expanded to 12 additional strains. The number of [^{3}H]cytisine binding sites and $^{86}Rb^{+}$ efflux stimulated by 10 μM nicotine were determined in the same eight brain regions as were analyzed in the 129 and A strains. The binding results for these strains, plus the results obtained with the A and 129SvEv strains, are presented in Table 1. The data obtained in seven of the brain regions (septum was deleted from these analyses because of sample pooling) were analyzed using two-way ANOVA; septal data were analyzed separately using a one-way ANOVA. The two-way ANOVA of the [^{3}H]cytisine binding data detected significant effects of brain region, mouse strain, and a significant region-by-strain interaction (statistical results are given in Table 1). The one-way ANOVA of the

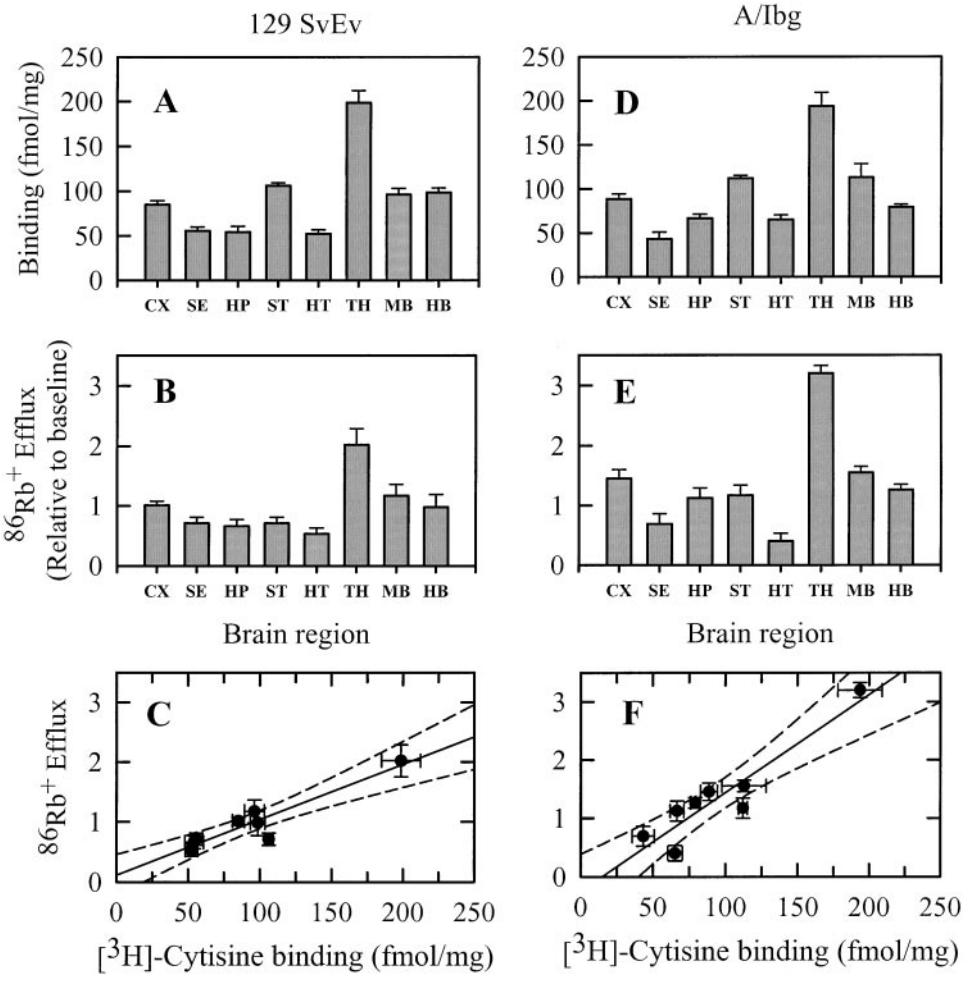

Fig. 3. Comparison of [^{3}H]cytisine binding and $^{86}Rb^{+}$efflux for A/J and 129 SvEv mice. A, B, and C, results for binding, efflux, and the correlation between these two measures for 129 SvEv mice. D, E, and F, results for binding, efflux, and the binding-efflux correlation for A/J mice. For 129 SvEv mice, significant differences were seen for binding ($F_{6,30} = 50.54$, $p < 0.001$; A) and efflux ($F_{6,24} = 15.21$, $p < 0.001$; B), and the correlation of efflux and binding was significant ($r = 0.94$, $p < 0.01$; C). For A/Ibg mice, significant differences were seen for binding ($F_{6,30} = 27.46$, $p < 0.001$; D) and efflux ($F_{6,24} = 71.41$, $p < 0.001$; E) with a significant correlation between binding and efflux ($r = 0.93$, $p < 0.01$; F). Two-way ANOVA for binding revealed a significant effect of region ($F_{6,60} = 71.88$, $p < 0.001$) but no effect of strain. Two-way ANOVA for efflux revealed a significant effect for region ($F_{6,48} = 68.01$, $p < 0.0018$) and strain ($F_{1,8} = 7.53$, $p = 0.05$). A significant strain-by-region interaction was seen also ($F_{6,48} = 4.90$, $p < 0.001$).

septal binding data did not detect a significant effect of strain (see Table 1 for statistical results).

Table 2 presents the results for the strain-by-region analysis of nicotine-stimulated $^{86}Rb^{+}$ efflux. The two-way ANOVA of the data obtained in the seven brain regions detected significant effects of brain region, mouse strain, and a significant strain-by-region interaction. The one-way ANOVA of the septal data detected a significant effect of strain (see Table 2 for statistical results).

The data presented in Fig. 3, C and F indicate that, within a mouse strain, variability in regional nicotine-stimulated $^{86}Rb^{+}$ flux is significantly correlated with regional differences in the number of [^{3}H]cytisine binding sites. Consequently, this analysis was done for all of the strains using data reported in Tables 1 and 2. The results of these correlational analyses are reported in Fig. 4. The correlation between [^{3}H]cytisine binding and ion flux in the eight brain regions ranged between 0.89 (DBA/2) and 0.99 (BALB/c) and was significant for every strain. In all cases, 80% or more of the variation in nicotine-stimulated $^{86}Rb^{+}$ efflux across brain regions within a mouse strain could be accounted for by differences in the number of [^{3}H]cytisine binding sites. Thus, within a mouse strain, nicotine-stimulated ion flux increased across brain regions along with increases in the number of [^{3}H]cytisine binding sites.

An entirely different result was obtained when the relationship between binding and ion flux was compared across strains within brain region (data not shown). Binding and ion flux were not significantly correlated in any of the brain regions except for striatum ($r = -0.63$), where a significant, weak negative correlation between binding and ion flux was observed. Thus, an increase in binding sites did not result in an increase in nicotine-stimulated ion flux across strains.

A potential explanation for the finding that the number of [^{3}H]cytisine binding sites did not covary with ion flux within brain regions across mouse strains is that the same binding site may vary in function across mouse strains. To compare receptor function across brain regions and mouse strains, the nicotine-stimulated $^{86}Rb^{+}$ efflux was normalized by dividing the ion flux by the amount of [^{3}H]cytisine binding. This value, which will be referred to from this point on as the functionality ratio, was calculated for each brain region in each mouse strain. The results of these calculations and the statistical analysis are reported in Table 3. Statistical analyses of the data obtained in the seven brain regions (septum excluded from the two-way ANOVA because tissue was pooled from several animals) detected significant influences of brain region and strain on the functionality ratio.

A recent report described a SNP in the Chrna4 gene between the LS and SS selected mouse lines (Stitzel et al., 2001). This SNP leads to an alanine/threonine variation at amino acid position 529 of the nicotinic receptor α4 subunit. To determine whether the differences in receptor function

TABLE 1

Regional [^{3}H]cytisine binding (femtomoles per milligram ± S.E.M.) in 14 inbred mouse strains

Statistical analysis (repeated-measures two-way ANOVA) revealed a significant effect of strain ($P = 0.0078$), region ($P < 0.000001$), and strain-region interaction ($P = 0.000003$).

	CX	SE	HP	ST	HT	TH	MB	HB
A	88.80 ± 5.84	43.40 ± 7.64	66.70 ± 4.74	112.15 ± 3.01	65.33 ± 5.03	193.72 ± 15.51	113.03 ± 15.31	79.33 ± 3.23
BALB	79.67 ± 5.97	44.85 ± 10.36	61.52 ± 4.34	93.12 ± 5.15	56.88 ± 4.33	205.73 ± 14.59	110.13 ± 5.92	91.57 ± 4.22
BUB	63.74 ± 3.67	38.89 ± 8.71	53.23 ± 3.00	93.77 ± 4.08	55.14 ± 4.36	162.13 ± 9.96	99.23 ± 11.64	81.67 ± 3.31
CBA	75.37 ± 6.35	37.63 ± 7.97	45.07 ± 4.63	95.10 ± 3.97	43.91 ± 5.52	163.10 ± 5.10	100.11 ± 10.45	63.20 ± 4.08
C3H/2	79.25 ± 3.66	36.42 ± 4.66	57.47 ± 5.75	93.20 ± 4.42	53.95 ± 7.53	176.95 ± 6.69	106.12 ± 8.39	63.17 ± 4.86
C57 BL/6	89.40 ± 4.80	43.30 ± 3.69	63.02 ± 6.57	100.73 ± 4.86	60.90 ± 6.05	201.50 ± 12.25	126.52 ± 6.89	77.38 ± 6.19
C57 BL/10	87.89 ± 7.08	36.80 ± 6.48	60.36 ± 4.03	104.11 ± 6.44	58.37 ± 7.94	199.37 ± 10.13	97.50 ± 6.02	82.80 ± 3.24
C57 BR	82.93 ± 4.55	47.98 ± 7.34	62.72 ± 7.93	91.23 ± 6.52	53.52 ± 4.64	168.95 ± 16.19	104.88 ± 10.61	67.48 ± 11.70
C58	87.13 ± 5.74	46.97 ± 10.37	59.69 ± 4.49	100.84 ± 6.89	60.01 ± 2.84	198.10 ± 8.43	103.83 ± 9.46	75.07 ± 6.90
DBA/2	87.07 ± 6.75	48.70 ± 5.67	51.78 ± 11.96	106.58 ± 5.32	57.28 ± 11.98	181.37 ± 7.71	91.72 ± 4.76	68.25 ± 3.33
129	85.07 ± 4.17	55.80 ± 4.37	54.32 ± 6.56	106.25 ± 3.00	52.45 ± 4.25	198.68 ± 13.70	96.28 ± 6.93	98.57 ± 5.12
AKR	63.62 ± 7.90	48.18 ± 20.14	49.51 ± 4.74	84.69 ± 11.91	54.68 ± 11.06	173.96 ± 21.26	100.37 ± 7.20	91.40 ± 10.12
DBA 1	77.27 ± 1.80	48.17 ± 6.75	59.22 ± 3.26	88.81 ± 4.63	48.95 ± 9.76	220.05 ± 10.40	140.92 ± 15.40	98.51 ± 8.92
RIII	74.75 ± 10.89	41.06 ± 12.70	65.44 ± 8.66	58.20 ± 7.00	25.91 ± 5.62	145.29 ± 21.10	125.07 ± 12.94	83.69 ± 22.53

TABLE 2

Regional nicotine-stimulated $^{86}Rb^{+}$ efflux (E_{max} ± S.E.M.) in 14 inbred mouse strains

Statistical analysis (repeated-measures ANOVA) revealed a significant effect of strain ($P = 0.000007$), region ($P < 0.000001$), and also a significant strain-by-region interaction ($P = 0.000001$).

	CX	SE	HP	ST	HT	TH	MB	HB
A	1.45 ± 0.15	0.69 ± 0.17	1.12 ± 0.17	1.17 ± 0.17	0.40 ± 0.13	3.20 ± 0.13	1.55 ± 0.10	1.26 ± 0.09
BALB	0.97 ± 0.20	0.40 ± 0.10	0.64 ± 0.14	0.87 ± 0.19	0.68 ± 0.13	2.47 ± 0.24	1.24 ± 0.28	0.94 ± 0.13
BUB	1.14 ± 0.09	0.44 ± 0.08	0.78 ± 0.13	1.02 ± 0.13	0.43 ± 0.05	2.17 ± 0.31	1.37 ± 0.21	0.90 ± 0.15
CBA	1.15 ± 0.16	0.50 ± 0.14	0.76 ± 0.11	0.81 ± 0.13	0.41 ± 0.07	2.12 ± 0.24	1.03 ± 0.05	0.99 ± 0.18
C3H/2	1.37 ± 0.11	0.61 ± 0.16	0.96 ± 0.10	1.05 ± 0.06	0.76 ± 0.16	2.80 ± 0.16	1.49 ± 0.12	1.26 ± 0.14
C57 BL/6	1.22 ± 0.13	0.54 ± 0.12	1.04 ± 0.12	1.25 ± 0.16	0.61 ± 0.07	2.10 ± 0.21	1.27 ± 0.16	1.24 ± 0.10
C57 BL/10	1.40 ± 0.17	0.46 ± 0.06	0.91 ± 0.09	1.21 ± 0.09	0.63 ± 0.06	1.95 ± 0.20	1.35 ± 0.24	1.26 ± 0.08
C57 BR	1.31 ± 0.12	0.47 ± 0.14	0.81 ± 0.08	1.25 ± 0.17	0.60 ± 0.06	2.41 ± 0.28	1.91 ± 0.27	1.15 ± 0.15
C58	1.09 ± 0.08	0.56 ± 0.08	0.73 ± 0.08	0.96 ± 0.08	0.73 ± 0.08	2.23 ± 0.23	1.56 ± 0.14	1.14 ± 0.08
DBA/2	1.11 ± 0.11	0.56 ± 0.28	1.00 ± 0.11	0.97 ± 0.14	0.99 ± 0.27	2.10 ± 0.14	1.38 ± 0.15	1.09 ± 0.11
129	1.01 ± 0.07	0.71 ± 0.10	0.66 ± 0.11	0.71 ± 0.10	0.53 ± 0.10	2.02 ± 0.27	1.17 ± 0.19	0.98 ± 0.21
AKR	1.44 ± 0.10	1.07 ± 0.24	1.23 ± 0.16	1.63 ± 0.17	1.25 ± 0.11	2.71 ± 0.16	2.17 ± 0.35	1.49 ± 0.18
DBA 1	1.23 ± 0.09	1.00 ± 0.15	1.35 ± 0.16	1.57 ± 0.11	1.09 ± 0.10	2.93 ± 0.14	2.62 ± 0.15	1.74 ± 0.19
RIII	1.28 ± 0.17	0.84 ± 0.17	1.04 ± 0.11	1.44 ± 0.09	0.92 ± 0.16	2.25 ± 0.23	2.19 ± 0.20	1.57 ± 0.15

across inbred mouse strains might be related to these α4 subunit variants, the Chrna4 A529T genotype was evaluated in each of the 14 inbred strains as described under *Experimental Procedures* (Fig. 5). Eight of the strains carry the Thr-529 variant of Chrna4 and six of the strains carry the Ala-529 variant. As expected, closely related strains were identical with regard to Chrna4 genotype. For example, all members of the C57 family (C57BL/6, C57BL/10, C57BR, and C58) carry the same allele (Thr-529), and both members of the DBA family are identical (Ala-529). Figure 6 presents an analysis of the effects of the Chrna4 polymorphism on $^{86}Rb^+$ efflux (top), [^{3}H]cytisine binding (middle), and functionality ratio (bottom). Significant overall effects of the Chrna4 polymorphism on ion flux were detected in seven of the eight brain regions (statistical analyses are presented in the legend to Fig. 6). In all of the brain regions except cortex, the mean nicotine-stimulated ion flux was greater for those strains that have the alanine-containing α4 subunit. In contrast, the Chrna4 polymorphism did not seem to influence [^{3}H]cytisine binding, with the possible exception of striatum, where binding was slightly but significantly higher in those strains that carry the threonine-containing variant of Chrna4. The mean value of the functionality ratio was significantly higher in those strains that carry the Ala-529 variant of Chrna4 in all of the brain regions except striatum.

Discussion

The experiments reported here replicate and extend the observation that nicotine-stimulated $^{86}Rb^+$ efflux is significantly correlated ($r > 0.9$) with the number of [^{3}H]nicotine binding sites across brain regions (Marks et al., 1993). This observation suggests that the major receptor responsible for the nicotine-stimulated $^{86}Rb^+$ efflux is the same receptor that binds agonists, such as [^{3}H]nicotine and [^{3}H]cytisine, with high affinity. This receptor presumably includes α4 and β2 subunits because[^{3}H]nicotine binding is lost in nearly all brain regions, including those used in our studies, in α4

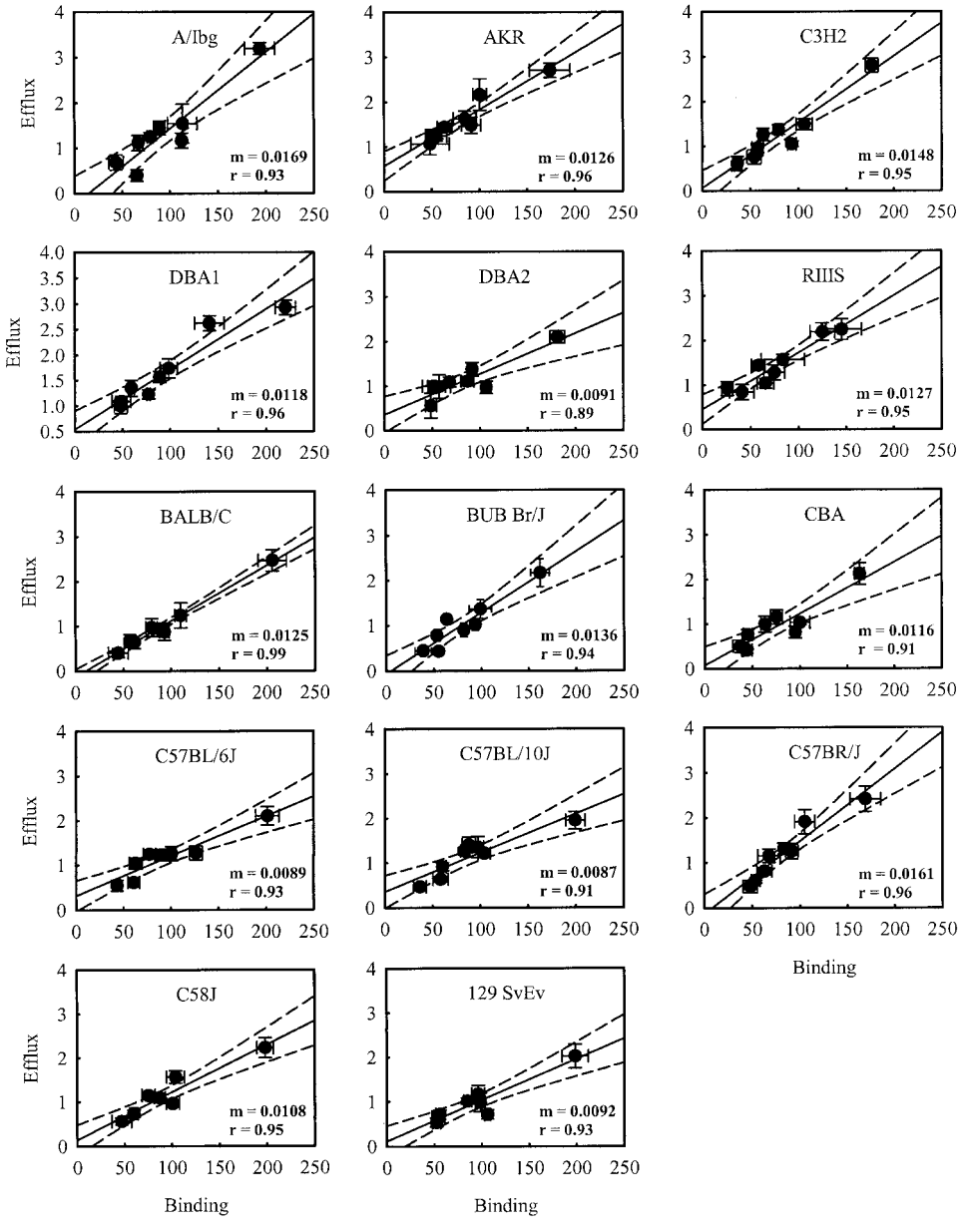

Fig. 4. Correlation of $^{86}Rb^+$ efflux and [^{3}H]cytisine binding for the 14 inbred strains. Efflux and binding for the eight brain regions correlated significantly for all 14 mouse strains. The slopes (m) and correlation coefficients (r) for each strain are presented.

MOL PHARM
MOLECULAR PHARMACOLOGY
aspet

TABLE 3
Regional functionality ratio [maximal $^{86}Rb^{+}$ efflux/[^{3}H]cytisine binding (femtomoles per milligram)] in 14 inbred mouse strains
Statistical analyses (two-way ANOVA) of the data obtained in seven brain regions (septum excluded from analysis because tissue was pooled from several animals) detected significant influences of brain region ($P < 0.0001$) and strain ($P < 0.05$) on the functionality ratio.

	CX	SE	HP	ST	HT	TH	MB	HB
A	0.0163 ± 0.0020	0.0159 ± 0.0048	0.0168 ± 0.0028	0.0104 ± 0.0015	0.0061 ± 0.0020	0.0165 ± 0.0015	0.0137 ± 0.0021	0.0159 ± 0.0013
BALB	0.0122 ± 0.0027	0.0089 ± 0.0030	0.0104 ± 0.0024	0.0093 ± 0.0021	0.0120 ± 0.0025	0.0120 ± 0.0014	0.0113 ± 0.0026	0.0103 ± 0.0015
BUB	0.0179 ± 0.0017	0.0113 ± 0.0033	0.0147 ± 0.0026	0.0109 ± 0.0015	0.0078 ± 0.0011	0.0134 ± 0.0021	0.0138 ± 0.0027	0.0110 ± 0.0019
CBA	0.0153 ± 0.0025	0.0133 ± 0.0047	0.0169 ± 0.0030	0.0085 ± 0.0014	0.0093 ± 0.0020	0.0130 ± 0.0015	0.0103 ± 0.0012	0.0157 ± 0.0030
C3H	0.0173 ± 0.0016	0.0167 ± 0.0049	0.0167 ± 0.0024	0.0113 ± 0.0008	0.0141 ± 0.0036	0.0158 ± 0.0011	0.0140 ± 0.0016	0.0199 ± 0.0027
C57BL/6	0.0136 ± 0.0016	0.0125 ± 0.0030	0.0165 ± 0.0026	0.0124 ± 0.0017	0.0100 ± 0.0015	0.0104 ± 0.0012	0.0100 ± 0.0014	0.0160 ± 0.0018
C57BL/10	0.0159 ± 0.0023	0.0125 ± 0.0027	0.0151 ± 0.0018	0.0116 ± 0.0011	0.0108 ± 0.0011	0.0098 ± 0.0011	0.0138 ± 0.0026	0.0152 ± 0.0011
C57BR	0.0158 ± 0.0017	0.0098 ± 0.0033	0.0129 ± 0.0021	0.0137 ± 0.0021	0.0112 ± 0.0015	0.0143 ± 0.0021	0.0182 ± 0.0032	0.0170 ± 0.0037
C 58	0.0125 ± 0.0012	0.0119 ± 0.0031	0.0122 ± 0.0016	0.0095 ± 0.0010	0.0122 ± 0.0015	0.0113 ± 0.0013	0.0150 ± 0.0019	0.0152 ± 0.0018
DBA 2	0.0127 ± 0.0016	0.0115 ± 0.0059	0.0193 ± 0.0049	0.0091 ± 0.0014	0.0173 ± 0.0059	0.0116 ± 0.0009	0.0150 ± 0.0018	0.0160 ± 0.0018
129 SvEv	0.0119 ± 0.0010	0.0127 ± 0.0021	0.0122 ± 0.0025	0.0067 ± 0.0010	0.0101 ± 0.0021	0.0102 ± 0.0015	0.0122 ± 0.0022	0.0099 ± 0.0022
AKR	0.0226 ± 0.0032	0.0222 ± 0.0105	0.0248 ± 0.0040	0.0192 ± 0.0034	0.0229 ± 0.0051	0.0156 ± 0.0021	0.0216 ± 0.0038	0.0183 ± 0.0032
DBA 1	0.0159 ± 0.0012	0.0207 ± 0.0042	0.0228 ± 0.0030	0.0177 ± 0.0015	0.0222 ± 0.0049	0.0133 ± 0.0009	0.0186 ± 0.0023	0.0177 ± 0.0025
RIIIS	0.0171 ± 0.0034	0.0204 ± 0.0075	0.0159 ± 0.0027	0.0247 ± 0.0034	0.0355 ± 0.0099	0.0155 ± 0.0027	0.0175 ± 0.0024	0.0168 ± 0.0043

(Marubio et al., 1999) and β2 (Picciotto et al., 1995) null mutant mice. The fact that a significant correlation between binding and function were seen in each of the 14 inbred mouse strains examined supports the assertion that the same receptor that binds agonists with high affinity modulates the ion flux response.

Although a strong correlation between nicotine-stimulated $^{86}Rb^{+}$ and [^{3}H]cytisine binding was observed within inbred mouse strains, a significant correlation between these two measures was not observed when these data were compared across mouse strains within brain regions. This finding argues that variations in receptor numbers are not necessarily predictive of differences in receptor function between individuals. Moreover, this finding suggests that the functional properties of the receptor(s) that modulate the nicotine-stimulated ion flux response are not the same across mouse strains.

Some of this variability in nicotine-stimulated ion flux across mouse strains seems to be influenced by a missense polymorphism in the α4 subunit. This polymorphism leads to an alanine/threonine variation at amino acid position 529 (A529T) within the large cytoplasmic loop between transmembrane domains three and four. Effects of the polymorphism on receptor function were evident when the data were calculated in terms of maximal ion flux and in terms of the functionality ratio (flux per femtomole per milligram of pro-

Fig. 5. Chrna4 A529T genotype among 14 inbred mouse strains. A 405-base pair region of the Chrna4 locus containing the A529T SNP was amplified by PCR and screened for the A529T SNP by digestion with *Stu*I. Chrna4 PCR products that are digested by *Stu*I possess the Ala-529 codon of Chrna4, whereas those products that are not digested by *Stu*I possess the Thr-529 codon of Chrna4. *M* = 100-base pair ladder (Invitrogen, Carlsbad, CA).

tein of [^{3}H]cytisine binding sites). Dose-response analyses of nicotine-stimulated ion flux suggest that the A529T polymorphism alters maximal agonist-stimulated ion flux; agonist potency does not seem to be affected. These findings, initially observed in the inbred strains A/J and 129SvEv, were confirmed when nicotine-stimulated ion flux elicited by a maximally activating concentration of nicotine (10 μM) was measured in eight brain regions from 14 inbred mouse strains. The ion flux stimulated by this concentration of nicotine was significantly greater in seven of the eight brain regions in those mouse strains that carry the Ala-529 variant of the α4 subunit. This finding supports the assertion that the A529T polymorphism influences receptor function and also provides support for the suggestion that the receptor that modulates the $^{86}Rb^+$ efflux process is an $\alpha4\beta2$* type (Marks et al., 1993, 1996, 2000; Whiteaker et al., 2000).

The A529T polymorphism was originally identified in two mouse lines that were selectively bred for long and short ethanol-induced sleep time, or duration of loss of the righting response (Stitzel et al., 2001). LS-SS differences in nicotine-stimulated $^{86}Rb^+$ efflux from thalamic synaptosomes were not found using the assay conditions used in the studies reported here. This finding does not, however, disagree with findings obtained in the current study. Nicotine-stimulated ion flux is probably affected by several factors that may vary across mouse strains. Therefore, measuring potential effects of a polymorphism on ion flux is risky when only two strains are used. This assertion is supported by the studies reported here because when a larger number of strains were tested, an overall effect of the polymorphism was observed. Parenthetically, LS-SS differences in nicotine-stimulated $^{86}Rb^+$ efflux were observed when BSA was removed from the perfusion buffer; maximal nicotine-stimulated ion flux was greater in LS thalamic synaptosomes (Stitzel et al., 2001). A potential explanation for this finding is provided by the studies of Gurantz et al. (1993), who noted that BSA enhanced the function of chick ciliary ganglia nicotinic receptors. Gurantz et al. concluded that BSA alters the ratio of ground state (activatable) to desensitized receptors, perhaps via an effect on desensitization processes. Thus, the finding that the addition of BSA alters the apparent effects of the A/T polymorphism on nicotine-stimulated $^{86}Rb^+$ efflux suggests that the polymorphism may regulate receptor dynamics, such as the ratio of ground state/desensitized receptors or desensitization rates.

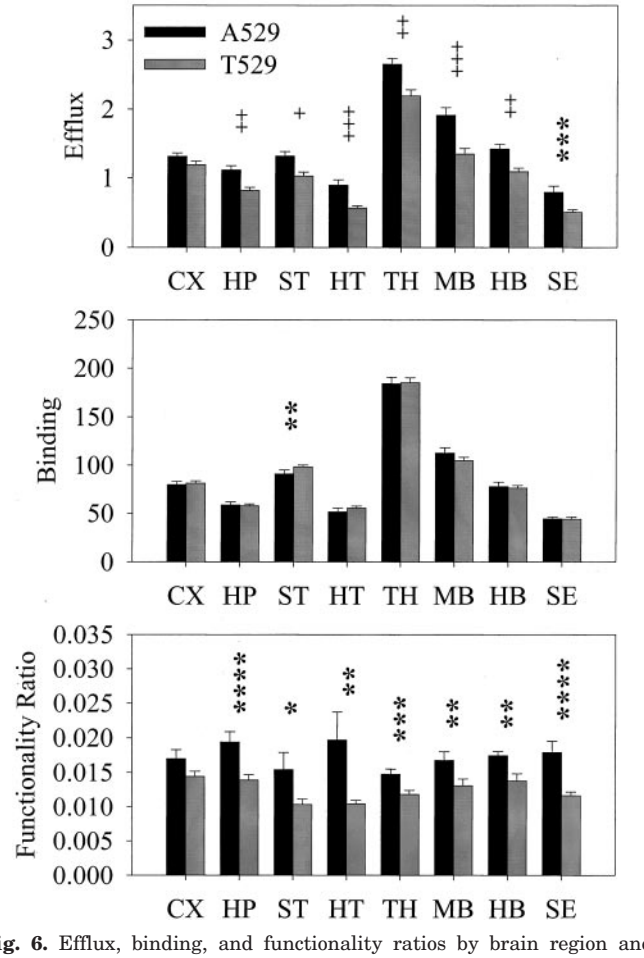

Fig. 6. Efflux, binding, and functionality ratios by brain region and polymorphism. Top and middle, efflux and binding results by brain region and polymorphism. Significant effects of the A529T polymorphism were seen for efflux for all regions except cortex. No significant effects were seen for binding with the exception of the striatum. Bottom, functionality ratio results by brain region and polymorphism. Significant effects of the polymorphism were seen for all brain regions with the exception of the cortex. ⋆, $p = 0.05$; ⋆⋆, $p < 0.05$; ⋆⋆⋆, $p < 0.01$; ⋆⋆⋆⋆, $p < 0.005$; +, $p < 0.001$; ++, $p < 0.0005$; +++, $p < 0.0001$ (two-tailed Student's t test).

Studies using nAChR subunit chimeras have identified potential roles for the extracellular domain in regulating sensitivity to agonists (Figl et al., 1992; Luetje et al., 1993; Corringer et al., 1998) and antagonists (Harvey et al., 1996), but this approach has not yielded much information about the role of the cytoplasmic loop in regulating neuronal nAChR function. One exception to this is a study done by Gross et al. (1991), who detected a potential function for the cytoplasmic loop in a study that used $\alpha4/\alpha3$ (residues 1–200 of α4 and 196–474 of α3) and $\alpha3/\alpha4$ (residues 1–195 of α3 and 201–599 of α4) chimeras. The N-terminal region of each chimera was uniquely responsible for regulating acetylcholine-induced receptor activation, whereas components in both regions of the chimera played a role in regulating the rate of receptor desensitization. Using chimeric nAChR subunit constructs, Williams et al. (1998) also demonstrated that the large cytoplasmic loop is critical for subunit-type specific receptor trafficking.

Although the molecular basis for the effect of the Chrna4 A529T polymorphism on receptor function has not been established, amino acid sequence-based searches have identified potential phosphorylation sites at the site of, or adjacent to, the polymorphism. According to a phosphorylation site prediction algorithm (http://www.cbs.dtu.dk/databases/PhosphoBase/predict/predict.html), a threonine at amino acid position 529 may serve as a substrate for casein kinase I. In addition, the serine (Ser-530) that is immediately carboxyl-terminal to the A529T polymorphism [DQ (T/A) **S***PCK] may be a substrate for the cdc2 family of kinases that includes Cdk5. Phosphorylation of neuronal nAChRs has been shown to influence receptor desensitization or recovery from desensitization (Downing and Role, 1987; Khiroug et al., 1998; Nishizaki and Sumikawa, 1998; Paradiso and Brehm, 1998; Fenster et al., 1999) and may affect receptor trafficking (Haselbeck and Berg, 1996). Therefore, the differences in receptor function observed between the A529T variants of the α4 subunit might be explained by differential phosphorylation at or near the site of the polymorphism.

In addition to being a potential substrate for phosphoryla-

tion, the region around the α4 subunit polymorphism has strong "loop" character (non-α helix, non-β sheet) according to a variety of secondary structure prediction algorithms (http://www.embl-heidelberg.de/predictprotein/predictprotein.html). However, the loop character of this region was found to be greater when alanine is located at position 529. This information suggests that the Ala-529 and Thr-529 variants of the α4 subunit in mice may have altered secondary structure in the vicinity of the polymorphism. This may be of importance because the α helixes in this portion of the cytoplasmic loop may serve as a filter that affects cation flux by excluding anions and other impermeant species from the vicinity of the ion pore (Miyazawa et al., 1999).

Previous studies have shown that variability in the number of [^{3}H]L-nicotine binding sites in mouse brain is predictive of inbred mouse strain differences in sensitivity to several behavioral and physiological responses to nicotine (Marks et al., 1989). The observation that mouse strains also vary in nicotine-stimulated $^{86}Rb^+$ efflux suggests that receptor function may also contribute to individual differences in sensitivity to nicotine. In support of this possibility, Chrna4 polymorphisms have been shown to be associated with mouse strain differences in sensitivity to various responses to nicotine (Stitzel et al., 2000; Tritto et al., 2002). Therefore, further studies to evaluate the effect of individual differences in nicotine-stimulated ion flux on variability in sensitivity to nicotine should be conducted.

In summary, the experiments reported here yielded results that demonstrate that inbred mouse strains differ in nicotine-stimulated $^{86}Rb^+$ efflux and indicate that a naturally occurring polymorphism in the α4 nicotinic receptor subunit influences these strain differences in receptor function. This finding also supports the suggestion that the major nicotinic receptor that modulates the ion flux response includes an α4 subunit. It is not known how the polymorphism exerts its effect, but several hypotheses have been proposed that may be testable using available methodologies.

References

Buisson B, Gopalakrishnan M, Arneric SP, Sullivan JP, and Bertrand D (1996) Human $\alpha4\beta2$ neuronal nicotinic acetylcholine receptor in HEK 293 cells: a patch-clamp study. *J Neurosci* **16:**7880–7891.

Corringer PJ, Bertrand S, Bohler S, Edelstein SJ, Changeux JP, and Bertrand D (1998) Critical elements determining diversity in agonist binding and desensitization of neuronal nicotinic acetylcholine receptors. *J Neurosci* **18:**648–657.

de Fiebre CM and Collins AC (1988) Decreased sensitivity to nicotine-induced seizures as a consequence of nicotine pretreatment in long-sleep and short-sleep mice. *Alcohol* **5:**55–61.

Downing JE and Role LW (1987) Activators of protein kinase C enhance acetylcholine receptor desensitization in sympathetic ganglion neurons. *Proc Natl Acad Sci USA* **84:**7739–7743.

Fenster CP, Beckman ML, Parker JC, Sheffield EB, Whitworth TL, Quick MW, and Lester RA (1999) Regulation of alpha4beta2 nicotinic receptor desensitization by calcium and protein kinase C. *Mol Pharmacol* **55:**432–443.

Figl A, Cohen BN, Quick MW, Davidson N, and Lester HA (1992) Regions of beta 4.beta 2 subunit chimeras that contribute to the agonist selectivity of neuronal nicotinic receptors. *FEBS Lett* **308:**245–248.

Flores CM, Rogers SW, Pabreza LA, Wolfe BB, and Kellar KJ (1992) A subtype of nicotinic cholinergic receptor in rat brain is composed of $\alpha4$ and $\beta2$ subunits and is up-regulated by chronic nicotine treatment. *Mol Pharmacol* **41:**31–37.

Flores CM, Wilson SG, and Mogil JS (1999) Pharmacogenetic variability in neuronal nicotinic receptor-mediated antinociception. *Pharmacogenetics* **9:**619–625.

Gross A, Ballivet M, Rungger D, and Bertrand D (1991) Neuronal nicotinic acetylcholine receptors expressed in *Xenopus* oocytes: role of the α subunit in agonist sensitivity and desensitization. *Eur J Physiol* **419:**545–551.

Gurantz D, Margiotta JF, Harootunian AT, and Dionne VE (1993) Modulation by albumin of neuronal cholinergic sensitivity. *Mol Pharmacol* **43:**807–812.

Harvey SC, Maddox FN, and Luetje CW (1996) Multiple determinants of dihydro-beta-erythroidine sensitivity on rat neuronal nicotinic receptor alpha subunits. *J Neurochem* **67:**1953–1959.

Haselbeck RC and Berg DK (1996) Tyrosine kinase inhibitors alter composition of nicotinic receptors on neurons. *J Neurobiol* **31:**404–414.

Hatchell PC and Collins AC (1977) Influences of genotype and sex on behavioral tolerance to nicotine in mice. *Pharmacol Biochem Behav* **6:**25–30.

Khiroug L, Sokolova E, Giniatullin R, Afzalov R, and Nistri A (1998) Recovery from desensitization of neuronal nicotinic acetylcholine receptors of rat chromaffin cells is modulated by intracellular calcium through distinct second messengers. *J Neurosci* **18:**2458–2466.

Luetje CW and Patrick J (1991) Both α- and β-subunits contribute to the agonist sensitivity of neuronal nicotinic acetylcholine receptors. *J Neurosci* **11:**837–845.

Luetje CW, Piattoni M, and Patrick J (1993) Mapping of ligand binding sites of neuronal nicotinic acetylcholine receptors using chimeric alpha subunits. *Mol Pharmacol* **44:**657–666.

Marks MJ, Campbell SM, Romm E, and Collins AC (1991) Genotype influences the development of tolerance to nicotine in the mouse. *J Pharmacol Exp Ther* **259:**392–402.

Marks MJ, Farnham DA, Grady SR, and Collins AC (1993) Nicotinic receptor function determined by stimulation of rubidium efflux from mouse brain synaptosomes. *J Pharmacol Exp Ther* **264:**542–552.

Marks MJ, Grady SR, Yang Y-M, Lippiello PM, and Collins AC (1994) Desensitization of nicotine-stimulated $^{86}Rb^+$ efflux from mouse brain synaptosomes. *J Neurochem* **63:**2125–2135.

Marks MJ, Robinson SF, and Collins AC (1996) Nicotinic agonists differ in activation and desensitization of $^{86}Rb^+$ efflux from mouse thalamic synaptosomes. *J Pharmacol Exp Ther* **277:**1383–1396.

Marks MJ, Stitzel JA, and Collins AC (1989) Genetic influences on nicotine responses. *Pharmacol Biochem Behav* **33:**667–678.

Marks MJ, Stitzel JA, Grady SR, Picciotto MR, Changeux J-P, and Collins AC (2000) Nicotinic-agonist stimulated $^{86}Rb^+$ efflux and [^{3}H]epibatidine binding of mice differing in $\beta2$ genotype. *Neuropharmacology* **39:**2632–2645.

Marks MJ, Whiteaker P, Calcaterra J, Stitzel JA, Bullock AE, Grady SR, Picciotto MR, Changeux JP, and Collins AC (1999) Two pharmacologically distinct components of nicotinic receptor-mediated rubidium efflux in mouse brain require the beta2 subunit. *J Pharmacol Exp Ther* **289:**1090–1103.

Marubio LM, del Mar Arroyo-Jimenez M, Cordero-Erausquin M, Lena C, Le Novere N, de Kerchove d'Exaerde A, Huchet M, Damaj MI, and Changeux J-P (1999) Reduced antinociception in mice lacking neuronal nicotinic receptor subunits. *Nature (Lond)* **398:**805–810.

Meliska CJ, Bartke A, McGlacken G, and Jensen RA (1995) Ethanol, nicotine, amphetamine and aspartame consumption and preferences in C57BL/6 and DBA/2 mice. *Pharmacol Biochem Behav* **50:**619–626.

Miner LL and Collins AC (1989) Strain comparison of nicotine-induced seizure sensitivity and nicotinic receptors. *Pharmacol Biochem Behav* **33:**469–475.

Miyazawa A, Fujiyoshi Y, Stowell M, and Unwin N (1999) Nicotinic acetylcholine receptor at 4.6 resolution: transverse tunnels in the channel wall. *J Mol Biol* **288:**765–786.

Nishizaki T and Sumikawa K (1998) Effects of PKC and PKA phosphorylation on desensitization of nicotinic acetylcholine receptors. *Brain Res* **812:**242–245.

Paradiso K and Brehm P (1998) Long-term desensitization of nicotinic acetylcholine receptors is regulated via protein kinase A-mediated phosphorylation. *J Neurosci* **18:**9227–9237.

Picciotto MR, Zoli M, Lena C, Bessis A, Lallemand Y, LeNovere N, Vincent P, Pich EM, Brulet P, and Changeux J-P (1995) Abnormal avoidance learning in mice lacking functional high-affinity nicotine receptor in the brain. *Nature (Lond)* **374:**65–67.

Robinson SF, Marks MJ, and Collins AC (1996) Inbred mouse strains vary in oral self-selection of nicotine. *Psychopharmacology* **124:**332–339.

Sabey K, Paradiso K, Zhang J, and Steinbach H (1999) Ligand binding and activation of rat nicotinic $\alpha4\beta2$ receptors stably expressed in HEK293 cells. *Mol Pharmacol* **55:**58–66.

Stitzel JA, Dobelis P, Jimenez M, and Collins AC (2001) LS and SS mice differ in nicotine-stimulated $^{86}Rb^+$ efflux and $\alpha4$ nicotinic receptor subunit cDNA sequence. *Pharmacogenetics* **11:**331–339.

Stitzel JA, Jimenez M, Marks MJ, Tritto T, and Collins AC (2000) Potential role of the alpha4 and alpha6 nicotinic receptor subunits in regulating nicotine-induced seizures. *J Pharmacol Exp Ther* **293:**67–74.

Tritto T, Stitzel JA, Marks MJ, and Collins AC (2002) Variability in response to nicotine in the LSxSS RI strains: potential role of polymorphisms in $\alpha4$ and $\alpha6$ nicotinic receptor subunit genes. *Pharmacogenetics* **12:**197–208.

Whiteaker P, Marks MJ, Grady SR, Lu Y, Picciotto MR, Changeux J-P, and Collins AC (2000) Pharmacological and null mutation approaches reveal nicotinic receptor diversity. *Eur J Pharmacol* **393:**123–135.

Whiting P and Lindstrom J (1987) Purification and characterization of a nicotinic acetylcholine receptor from rat brain. *Proc Natl Acad Sci USA* **84:**595–599.

Whiting P, Schoepfer R, Lindstrom J, and Priestley T (1991) Structural and pharmacological characterization of the major brain nicotinic acetylcholine receptor subtype stably expressed in mouse fibroblasts. *Mol Pharmacol* **40:**463–472.

Williams BM, Temburni MK, Levey MS, Bertrand S, Bertrand D, and Jacob MH (1998) The long internal loop of the alpha 3 subunit targets nAChRs to subdomains within individual synapses on neurons in vivo. *Nat Neurosci* **1:**557–562.

Address correspondence to: Jerry A. Stitzel, Ph.D., University of Michigan Medical Center, 1500 E. Medical Center Drive, CCGC 2140, Ann Arbor, MI 48109-0930. E-mail: stitzel@umich.edu